



Synthesis and evaluation of novel F-18 labeled fluoroarylvaline derivatives: Potential PET imaging agents for tumor detection

Yali Qiao^a, Yong He^a, Shuting Zhang^a, Guixia Li^a, Hang Liu^a, Jingli Xu^a, Xiao Wang^a, Chuanmin Qi^{a,*}, Cheng Peng^b

^a Key laboratory of Radiopharmaceuticals, College of Chemistry, Beijing Normal University, Beijing 100875, People's Republic of China

^b Center of PET, Xuan Wu Hospital, Beijing 100053, People's Republic of China

ARTICLE INFO

Article history:

Received 12 November 2008

Revised 15 February 2009

Accepted 6 March 2009

Available online 14 March 2009

Keywords:

Amino acids

F-18 labeled

Fluoroarylvaline derivatives

PET imaging agents

Tumor detection

ABSTRACT

Two F-18 labeled fluoroarylvaline derivatives, methyl 2-(2-[¹⁸F]fluoro-4-nitrobenzamido)-3-methylbutanoate ([¹⁸F]**1**, [¹⁸F]MFNBMB) and its corresponding acid 2-(2-[¹⁸F]fluoro-4-nitrobenzamido)-3-methylbutanoic acid ([¹⁸F]**2**, [¹⁸F]FNBMB), have been designed and synthesized, respectively, by our team. Meanwhile, we research on their biodistributions in mice model bearing S 180 tumor. Furthermore, we also carried out the biological evaluations of 2-[¹⁸F]fluoroethoxyglucose ([¹⁸F]FDG) and O-2-[¹⁸F]fluoroethyl-L-tyrosine (L-[¹⁸F]FET) in the same model for comparison with our targeting molecules [¹⁸F]**1** and [¹⁸F]**2**. Excitingly, the tumor/blood (T/Bl) and tumor/brain (T/Br) ratios were 2.91, 7.06 at 30 min, 3.44, 5.61 at 60 min post injection for [¹⁸F]**1**, 2.32, 13.30 for [¹⁸F]**2** at 30 min post injection, which were obviously superior to [¹⁸F]FDG and L-[¹⁸F]FET in the same model and demonstrated that [¹⁸F]**1** and [¹⁸F]**2**, especially [¹⁸F]**2**, were potential PET imaging agents for tumor detection.

© 2009 Elsevier Ltd. All rights reserved.

As one of the nuclear medicine imaging modalities, positron emission tomography (PET) possesses the highest resolution and makes tracer concentration in tissues quantified.¹ As we all know, [¹⁸F]FDG has been extensively applied for diagnosing brain and systemic tumors as an efficient PET radiotracer.² When it comes to brain tumors, however, [¹⁸F]FDG has high background uptake in normal brain tissues which can reduce tumor-to-brain ratios; on the other hand, it represents substantive uptake in inflammatory tissues.³ Consequently, [¹⁸F]FDG always demonstrates low T/Br ratios and cannot well distinguish tumors from inflammation, both of which limit its application in the field of brain tumor PET imaging. Hence, plentiful research on the development of novel PET radiotracers has been carried out aiming at supplementing [¹⁸F]FDG.⁴ Fortunately, researchers have discovered that multifarious radiolabeled amino acids generally have huge potential value in oncology, especially for brain tumors with PET imaging modality which may be better tumor-imaging agents than [¹⁸F]FDG.⁵ So far, efforts primarily have focused on radiolabeled nonnatural amino acids considering their improved metabolic stability over radiolabeled natural amino acids and comparatively simple interpretation of tracer kinetics. O-2-[¹⁸F]fluoroethyl-L-tyrosine (L-[¹⁸F]FET), as an analogue of tyrosine, has been developed and evaluated which proved to be a useful nonnatural amino acid PET radiotracer for

diagnosis of tumors with a high specificity, particularly for brain tumors.⁶

Mainly due to the longer half-time of ¹⁸F (110 min) compared with ¹¹C (20 min), fluorine-18 becomes a widely used PET radionuclide in radiopharmacy.^{5a} Thus, fluorine-18 labeled radiopharmaceuticals, particularly various ¹⁸F-labeled amino acids, have been designed and synthesized to evaluate their potential use as PET imaging agents for tumors. From a radiochemical synthesis perspective, however, to label amino acids with ¹⁸F is no easy work, especially for some aromatic substrates.^{7–9} Initially, tyrosine, for example, was directly labeled with ¹⁸F on its aromatic positions⁷ by electrophilic substitution reaction with [¹⁸F]AcOF or [¹⁸F]F₂, which usually has low radiochemical yield. Whereafter, Wester's team indirectly labeled tyrosine by introduction of a fluoroalkyl group to the aromatic position, successfully getting O-2-[¹⁸F]fluoroethyl-L-tyrosine (L-[¹⁸F]FET), which prolonged the labeling time, though improved its radiochemical yield to some degree.^{6a,b} Therefore, considering radiochemical factors, we designed and synthesized novel F-18 labeled fluoroarylvaline derivatives based on natural amino acid L-valine modified by 2,4-dinitrobenzoic acid. The primary reason for adopting 2,4-dinitrobenzoic acid to modify the natural amino acid is owing to the synthetically easy introduction of fluorine-18 at *ortho*-position of the 2,4-dinitrobenzamide precursor. In addition, on account of the influence of molecular structure on its lipophilic property, we respectively produced methyl 2-(2-[¹⁸F]fluoro-4-nitrobenzamido)-3-methylbutanoate ([¹⁸F]**1**, [¹⁸F]MFNBMB) and its corresponding acid

* Corresponding author. Tel.: +086 13681380097; fax: +086 010 58802075.

E-mail address: qicmin@sohu.com (C. Qi).

2-(2-[^{18}F]fluoro-4-nitrobenzamido)-3-methylbutanoic acid ([^{18}F]2, [^{18}F]FNBMB) to evaluate their potential use as PET tumor tracers. In this Letter, we report the synthesis and biological evaluation of two novel non-natural fluorine-substituted L-valine derivatives for tumor imaging, ester [^{18}F]1 and its corresponding acid [^{18}F]2. The biological properties of these new radiotracers were evaluated using in vivo uptake assays in mice bearing S 180 tumor. Moreover, we also carried out the biological evaluation experiments of 2-[^{18}F]fluorodeoxyglucose ([^{18}F]FDG) and O-2-[^{18}F]fluoroethyl-L-tyrosine (L-[^{18}F]FET) in the same model for comparison with our targeting molecules [^{18}F]1 and [^{18}F]2 (Fig. 1).

The precursor 2-(2,4-dinitrobenzamido)-L-valine methyl ester (**5**) used in this study was easily prepared in only two steps from natural amino acid L-valine (**3**) as shown in Scheme 1. L-valine methyl ester hydrochloride (**4**) was produced by the reaction of L-valine with slightly more SOCl_2 in MeOH at 0°C for 30 min, then at rt for 12 h, followed by removal of SOCl_2 and MeOH by evaporation and further purified by recrystallization in 80% yield. The precursor was synthesized using 1.5 equiv L-valine methyl ester hydrochloride (**4**) and 1.5 equiv triethylamine (TEA) dissolved in CH_2Cl_2 , mixed for 5 min, then added 1.0 equiv 2,4-dinitrobenzoic acid, 1.1 equiv *N*-hydroxybenzotriazole (HOBt) and 1.1 equiv *N,N*-dicyclohexylcarbodiimide (DCC) at 0°C for 30 min, raised to room temperature for 12 h, the mixture was filtrated, washed and isolated by flash column chromatography in 38% yield. F-19 substituted compound 2-(2-fluoro-4-nitrobenzamido)-L-valine methyl ester (**1**) was synthesized directly from the 2,4-dinitrobenzoic acid modified precursor using TBAF·3H₂O in DMF at 115°C for 20 min in 66% yield. Hydrolysis of compound **1** with LiOH in MeOH, subse-

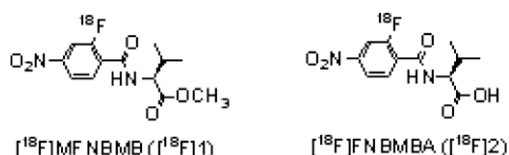
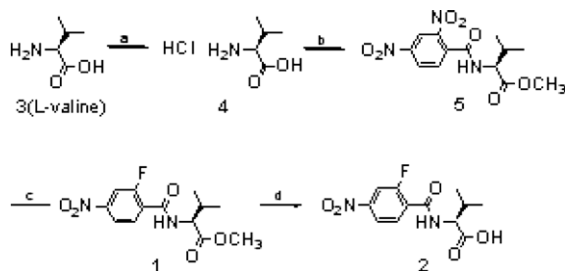
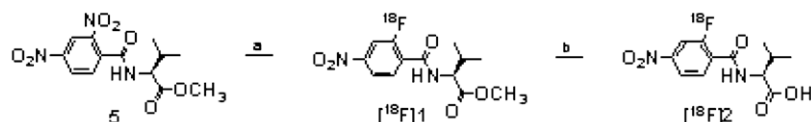


Figure 1. Structure of the F-18 labeled fluoroarylvaline derivatives used in this study.



Scheme 1. Synthesis of MFNBMB (**1**) and FNBMB (**2**). Experimental reagents and conditions: (a) SOCl_2 , MeOH, 0°C , 0.5 h, then rt, 12 h, 80%; (b) 2,4-dinitrobenzoic acid, TEA, HOBt, DCC, CH_2Cl_2 , 0°C , 0.5 h, then rt, 12 h, 38%; (c) TBAF·3H₂O, DMF, 115°C , 20 min, 66%; (d) (1) LiOH, MeOH, 0°C , 0.5 h, then rt, overnight, (2) 1 N HCl, 85%.



Scheme 2. Radiosynthesis of [^{18}F]MFNBMB ([^{18}F]1) and [^{18}F]FNBMB ([^{18}F]2). Experimental reagents and conditions: (a) K [^{18}F] F, Kryptofix 2.2.2., DMF, 115°C , 20 min, 30–40%; (b) (1) LiOH, MeOH, rt, 10 min, (2) 1 N HCl, >95%.

quent acidification with 1 N HCl and purification by recrystallization afforded its acid F-19 substituted compound 2-(2-fluoro-4-nitrobenzamido)-L-valine (**2**) in 85% yield (structure analysis data for **1** and **2** can be found in a Ref. 10).

The radiosynthesis of [^{18}F]MFNBMB and [^{18}F]FNBMB were performed beginning with the 2,4-dinitrobenzoic acid modified precursor by the nucleophilic substitution denitrofluorination reaction as shown in see Scheme 2. Fixation of K [^{18}F] F on Kryptofix_{2.2.2.} was used in the synthetic process. Optimal reaction conditions were obtained with a mixture of the precursor and the fluoride-Kryptofix_{2.2.2.} complex in 0.5 ml DMF at 115°C for 20 min in sealed conditions. The mixed product was highly diluted with water, adsorbed on a Sep-Pak Plus C18 cartridge and almost quantitatively desorbed with acetonitrile. Purification of the separated product was immediately executed by semi-preparative HPLC: Grace C18 column (250×4 mm i.d.); eluent: MeCN/H₂O = 70:30; flow rate: 3 ml/min; t_R (ester [^{18}F]1) = 7–10 min. After the separation and purification obtaining ester [^{18}F]1, hydrolysis using LiOH in MeOH at rt for only 10 min in open conditions and immediate acidification with 1 N HCl afforded [^{18}F]2 (t_R for acid [^{18}F]2 = 3–5 min). The pure compounds [^{18}F]1 and [^{18}F]2 were collected using physiological saline prepared for use in the biological evaluation experiment. The radiochemical yield is approximately 30–40% without decay correction. The radiochemical purity and chemical purity were >99%. Total labeling synthesis of [^{18}F]1 and [^{18}F]2 needed approximately 100 min.

On account of usage of natural amino acid L-valine as the initial material in the preparation of the precursor, we obtained two F-18 labeled L-[^{18}F]fluoroarylvaline derivatives in this study which were further confirmed by Radio-HPLC. After separation and purification, [^{18}F]MFNBMB ([^{18}F]1) was measured by Radio-HPLC showing a single peak at 7.3 min which matched well with its corresponding F-19 substituted MFNBMB (**1**, t_R = 7.0 min) within admissible error. As for [^{18}F]FNBMB ([^{18}F]2), single peak presented at 3.0 min, also matched well with FNBMB (**2**, t_R = 2.4 min).

Partition coefficients of the [^{18}F]MFNBMB and [^{18}F]FNBMB were determined by using 2.5 ml *n*-octanol as the organic phase and 2.5 ml 0.01 M PBS (pH 7.4) as water phase. After HPLC purification, 0.01 ml of [^{18}F]1 or [^{18}F]2 was added, mixed for 5 min and centrifuged for 5 min at room temperature. The radioactivity of equal volume of each phase was measured, respectively. The $\lg P$ of ester [^{18}F]1 was 0.58 and that of its corresponding acid [^{18}F]2 was –0.25.

The in vitro stability of [^{18}F]1 and [^{18}F]2 were tested by incubation of certain amounts of them in 0.9% NaCl, 0.01 M phosphate buffered saline (PBS) or 96% ethanol at room temperature up to 6 h and in organic solvents such as ethanol, DMF and MeCN at 60°C up to 30 min. According to TLC and HPLC, the compounds proved to be stable. No degradation or defluorination of them were observed.

The blood stability of [^{18}F]1 and [^{18}F]2 was evaluated in a tumor-bearing KM mouse, respectively. Thirty minutes after intravenous injection of 4 MBq of [^{18}F]1 and [^{18}F]2, the mouse was sacrificed. The blood was collected and immediately centrifuged for 5 min at 13,200 rpm. The supernatants of both centrifugation steps of blood were combined and passed through a C18 Sep-Pak cartridge. The cartridge was washed with 2 ml of water and eluted

with 2 ml of MeCN containing 0.1% TFA. After evaporation of the solvent, the residue was redissolved in 1 ml PBS and was injected onto the analytical HPLC. The compounds were stable in blood according to the analysis of HPLC.

The *in vivo* biological evaluation of [^{18}F]MFNBMB ([^{18}F]1) and [^{18}F]FNBMB ([^{18}F]2) were executed in female KM mice with S 180 tumor (animal experimental center, Peking University) weighing 20 ± 2 g on average. The experimental process were performed 14–18 days after inoculating the mouse with 5×10^6 tumor cells. The radiopharmaceuticals [^{18}F]1 or [^{18}F]2 radiosynthesized as mentioned above was solved in 100 μl saline solution and injected into the tail vein of awake mice subsequently placed into a small cage. The injected activities per animal ranged from 240 to 370 kBq. These injected doses of [^{18}F]1 or [^{18}F]2 were tracer doses without obvious pharmacological effects. The animals were sacrificed at 5 min, 15 min, 30 min, 60 min or 120 min after radiotracer injection, respectively. The tumor, brain and other organs to be examined were immediately removed, weighed and measured for F-18 radioactivity in a γ counter. The uptake of F-18 radioactivity in tissues and organs was expressed as percentage of injected dose per gram of tissue weight (%ID/g). The mean values were calculated from the individual measurements taking into account the background from the counter measurements and expressed at a precision of standard deviation (mean \pm SD, $n = 4$). The biological evaluation data of [^{18}F]MFNBMB and [^{18}F]FNBMB in mice bearing S 180 tumor were summarized in Tables 1 and 2, respectively.

In the distribution data of [^{18}F]1 shown as in Table 1, the radioactivity uptakes demonstrated an extremely rapid distribution and accumulation in all the tissues and organs at only 5 min after injection.

Obviously, uptakes in all the tissues and organs except for that in femur decreased as time elapsed. Uptake in femur peaked at 15 min post-injection and then reduced slightly with the lapse of time indicating the stabilization of [^{18}F]1 *in vivo*. Tumor had a relatively high initial radioactivity uptake representing approximately 2.78 ± 0.50 %ID/g, and decreased to 1.97 ± 0.47 %ID/g, still 71% radioactivity retained, showing certain retention in tumor. The blood uptake peaked immediately after injection, however, it decreased rapidly to only 22%, 9% radioactivity retained at 30 min, 60 min, respectively. The tumor-to-blood (T/BI) uptake ratio was 2.91 at 30 min and 3.44 at 60 min post-injection, meanwhile, the tumor-to-brain (T/Br) uptake ratio was 7.06 at 30 min and 5.61 at 60 min post-injection.

Compared with [^{18}F]1, its corresponding F-18 labeled acid [^{18}F]2 had significantly reduced uptakes in all tissues and organs, nevertheless, uptake of [^{18}F]2 still varied in the same way, that is to decrease in a time-dependent pattern. The difference of absolute radioactivity uptakes between the two F-18 labeled radiopharmaceuticals was mainly due to the discrepancy in their lipophilic properties. Initial tumor absolute uptake was 1.37 ± 0.68 %ID/g which minished approximately 50% compared with ester [^{18}F]1 in the same time point. Initial activity uptake in blood was 2.43 ± 0.53 %ID/g which was decreased by more than 20% based on [^{18}F]1 and reduced rapidly to only 10%, 6% radioactivity retained at 30 min, 60 min, respectively, which demonstrated a much faster and thorough clearance than ester [^{18}F]1. To our surprise, the tumor-to-brain (T/Br) uptake ratio reached a maximum 13.30 (much higher than [^{18}F]1) at 30 min post-injection, meanwhile, the tumor-to-blood (T/BI) uptake ratio was 2.32 at the same time point.

Table 1
Biodistribution data of [^{18}F]MFNBMB ([^{18}F]1) in mice bearing S 180 tumor^a

Organ	Time point (min)				
	5	15	30	60	120
Blood	3.09 \pm 0.38	2.18 \pm 0.12	0.68 \pm 0.04	0.28 \pm 0.06	0.19 \pm 0.02
Heart	1.35 \pm 0.57	0.60 \pm 0.22	0.40 \pm 0.28	0.19 \pm 0.01	0.08 \pm 0.02
Liver	15.90 \pm 0.66	8.60 \pm 0.34	3.66 \pm 0.23	0.27 \pm 0.03	0.14 \pm 0.02
Lung	5.49 \pm 0.17	2.57 \pm 0.34	1.31 \pm 0.25	0.31 \pm 0.01	0.25 \pm 0.11
Kidney	17.90 \pm 0.88	11.28 \pm 0.49	3.80 \pm 0.42	0.35 \pm 0.00	0.29 \pm 0.12
Femur	1.60 \pm 0.03	2.23 \pm 0.38	2.11 \pm 0.36	2.09 \pm 0.26	2.01 \pm 0.03
Muscle	1.43 \pm 0.34	1.39 \pm 0.23	0.82 \pm 0.06	0.69 \pm 0.13	0.58 \pm 0.00
Spleen	1.48 \pm 0.22	1.13 \pm 0.18	0.51 \pm 0.01	0.31 \pm 0.20	0.05 \pm 0.00
Brain	0.99 \pm 0.12	0.60 \pm 0.10	0.28 \pm 0.00	0.17 \pm 0.04	0.12 \pm 0.01
Tumor	2.78 \pm 0.50	2.06 \pm 0.84	1.97 \pm 0.47	0.95 \pm 0.07	0.31 \pm 0.11
Tumor/blood	0.90	0.94	2.91	3.44	1.67
Tumor/brain	2.79	342	7.06	5.61	2.61
Tumor/muscle	1.94	1.48	2.41	1.39	0.54

^a Values reported as means \pm SD ($n = 4$ at each time point).

Table 2
Biodistribution data of [^{18}F]FNBMB ([^{18}F]2) in mice bearing S 180 tumor^a

Organ	Time point (min)				
	5	15	30	60	120
Blood	2.43 \pm 0.53	1.27 \pm 0.19	0.24 \pm 0.01	0.15 \pm 0.03	0.06 \pm 0.00
Heart	1.07 \pm 0.89	0.72 \pm 0.84	0.29 \pm 0.02	0.11 \pm 0.08	0.05 \pm 0.07
Liver	6.54 \pm 0.03	3.35 \pm 0.42	1.59 \pm 0.78	0.77 \pm 0.06	0.50 \pm 0.01
Lung	5.04 \pm 0.66	2.01 \pm 0.07	1.38 \pm 0.03	1.14 \pm 0.06	0.57 \pm 0.01
Kidney	11.90 \pm 0.38	5.19 \pm 0.06	1.36 \pm 0.00	0.45 \pm 0.06	0.30 \pm 0.00
Femur	3.61 \pm 0.67	4.02 \pm 0.67	3.38 \pm 0.71	2.47 \pm 0.01	2.15 \pm 0.00
Muscle	0.99 \pm 0.19	0.47 \pm 0.20	0.21 \pm 0.02	0.15 \pm 0.02	0.12 \pm 0.04
Spleen	1.04 \pm 0.03	0.60 \pm 40.09	0.31 \pm 40.00	0.24 \pm 0.04	0.16 \pm 0.04
Brain	0.15 \pm 0.02	0.09 \pm 0.07	0.04 \pm 0.12	0.03 \pm 0.03	0.01 \pm 0.00
Tumor	1.37 \pm 0.68	0.91 \pm 0.12	0.56 \pm 0.01	0.27 \pm 0.14	0.08 \pm 0.07
Tumor/blood	0.56	0.72	2.32	1.83	1.30
Tumor/brain	9.38	10.40	13.30	9.99	6.90
Tumor/muscle	1.38	1.95	2.62	1.74	0.66

^a Values reported as means \pm SD ($n = 4$ at each time point).

For the purpose of better evaluating their potential use as PET tumor imaging agents, we executed the parallel biodistribution experiments of [^{18}F]FDG and L-[^{18}F]FET in the same animal model, data of which were displayed in Tables 3 and 4.

In biodistribution data of [^{18}F]FDG in Table 3, all tissues and organs demonstrated substantially lower radioactivity uptakes except for brain and tumor. For brain uptake, it achieved the maximum at 30 min, then continuously decreased till 120 min after injection. Evidently, uptake in brain had high values during all the experimental period. To certain degree, however, its [^{18}F]FDG's high background uptake in normal brain that resulted in the limitation of its application as a tumor imaging tracer, particularly for brain tumor. Tumor-to-brain uptake ratio was only 1.33 at 120 min post-injection. Besides, for biological data of L-[^{18}F]FET in Table 4, both brain and tumor uptakes maximized at 30 min and subsequently decreased with time elapsed. While, tumor-to-brain ratios varied from 2.10 to 2.95 and tumor-to-blood ratios was only slightly more than 1.00 at 30 min and still less than 2.00 at 120 min.

From the comparison of blood clearance rates as summarized in Figure 2, we can easily discover that radioactivity uptakes in blood of all F-18 labeled tracers ([^{18}F]1, [^{18}F]2, [^{18}F]FDG and L-[^{18}F]FET) were immediately peaked at 5 min post-injection and continuously decreased till 120 min post-injection. Obviously, both [^{18}F]1 and [^{18}F]2 had much lower absolute uptake values than L-[^{18}F]FET in blood from 5 min to 120 min post-injection. Moreover, compared with [^{18}F]FDG and L-[^{18}F]FET, the two radiotracers possessed much faster blood clearance velocity in which the blood uptake diminished to only 22% uptake retained for [^{18}F]1 and 10% for [^{18}F]2 at 30 min after injection. Furthermore, in the biodistribution data as

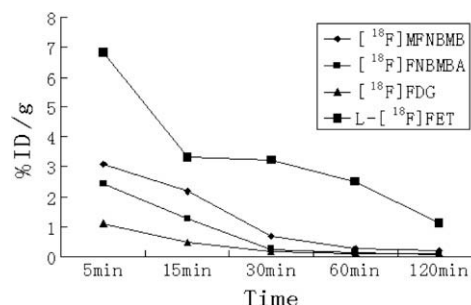


Figure 2. Comparison of blood clearance rates of [^{18}F]1 and [^{18}F]2 with those of [^{18}F]FDG and L-[^{18}F]FET together in the same animal model bearing S 180 tumor.

shown in Tables 1–4, the radioactivity uptake in tumor and brain peaked immediately at 5 min post-injection and continuously decreased till minimum for both [^{18}F]1 and [^{18}F]2 during all the experimental period. Dissimilarly, tumor and brain uptake of [^{18}F]FDG and L-[^{18}F]FET first increased then decreased with the lapse of time. Based on all these results, we summed up and compared tumor-to-brain uptake ratios of [^{18}F]1 and [^{18}F]2 with those of [^{18}F]FDG and L-[^{18}F]FET together in Figure 3. Patently, the T/Br ratios of compounds [^{18}F]1 (2.61_{min}–7.06_{max}) reached 7.06 as the maximum at 30 min post-injection which was much higher than the maximum (0.53_{min}–1.33_{max}) of [^{18}F]FDG (2.10_{min}–2.95_{max}) and that of L-[^{18}F]FET showing much potential value as one of PET tumor radiotracers. As for [^{18}F]2, tumor-to-brain ratios excitingly achieved 13.30 at 30 min after injection with 6.90 as the minimum at 120 min, which demonstrated excellent properties to be an efficient PET tumor imaging agent. In addition, maximums of T/BI (2.32), T/Br

Table 3
Biodistribution data of [^{18}F]FDG in mice bearing S 180 tumor^a

Organ	Time point (min)				
	5	15	30	60	120
Blood	1.09 ± 0.74	0.46 ± 0.14	0.16 ± 0.01	0.11 ± 0.05	0.11 ± 0.13
Heart	2.60 ± 0.06	2.50 ± 0.06	2.69 ± 0.14	3.24 ± 0.20	6.27 ± 0.30
Liver	1.35 ± 0.42	0.47 ± 0.17	0.23 ± 0.00	0.22 ± 0.04	0.20 ± 0.03
Lung	1.52 ± 0.66	0.77 ± 0.13	0.64 ± 0.05	0.57 ± 0.06	0.52 ± 0.11
Kidney	2.16 ± 0.35	1.04 ± 0.21	0.61 ± 0.23	0.54 ± 0.15	0.25 ± 0.06
Muscle	1.56 ± 0.13	1.14 ± 0.23	1.07 ± 0.86	0.97 ± 0.66	0.78 ± 0.06
Spleen	1.31 ± 0.40	0.95 ± 0.01	0.90 ± 0.19	0.83 ± 0.04	0.78 ± 0.18
Brain	2.40 ± 0.28	2.63 ± 0.10	3.07 ± 0.11	2.11 ± 0.17	1.28 ± 0.08
Tumor	1.27 ± 0.54	1.56 ± 0.23	1.86 ± 0.18	2.16 ± 0.34	1.70 ± 0.06
Tumor/blood	1.17	3.42	11.38	19.47	15.85
Tumor/brain	0.53	0.59	0.61	1.02	1.33
Tumor/muscle	0.81	1.37	1.75	2.23	2.20

^a Values reported as means ± SD (n = 4 at each time point).

Table 4
Biodistribution data of L-[^{18}F]FET in mice bearing S 180 tumor^a

Organ	Time point (min)				
	5	15	30	60	120
Blood	6.81 ± 0.95	3.30 ± 0.25	3.23 ± 0.33	2.51 ± 0.36	1.12 ± 0.21
Heart	5.89 ± 1.23	3.41 ± 0.31	3.27 ± 0.37	3.14 ± 0.26	0.94 ± 0.36
Liver	7.67 ± 1.34	5.60 ± 0.30	4.23 ± 0.28	3.56 ± 0.29	1.22 ± 0.51
Lung	16.80 ± 2.98	9.82 ± 0.45	8.57 ± 0.63	4.70 ± 0.41	1.55 ± 0.73
Kidney	6.58 ± 0.84	6.79 ± 0.23	2.38 ± 0.43	3.75 ± 0.49	1.25 ± 0.21
Muscle	2.88 ± 1.33	3.34 ± 0.41	2.69 ± 0.96	2.37 ± 0.38	2.10 ± 1.33
Spleen	3.34 ± 0.51	5.42 ± 0.31	1.16 ± 0.61	3.37 ± 0.34	1.22 ± 0.37
Brain	0.99 ± 0.24	1.03 ± 0.12	1.29 ± 0.09	0.94 ± 0.23	0.73 ± 0.21
Tumor	2.08 ± 0.49	2.50 ± 0.23	3.28 ± 0.69	2.75 ± 0.36	2.15 ± 1.36
Tumor/blood	0.31	0.76	1.02	1.10	1.92
Tumor/brain	2.10	2.43	2.54	2.93	2.95
Tumor/muscle	0.72	0.75	0.62	1.23	1.40

^a Values reported as means ± SD (n = 4 at each time point).

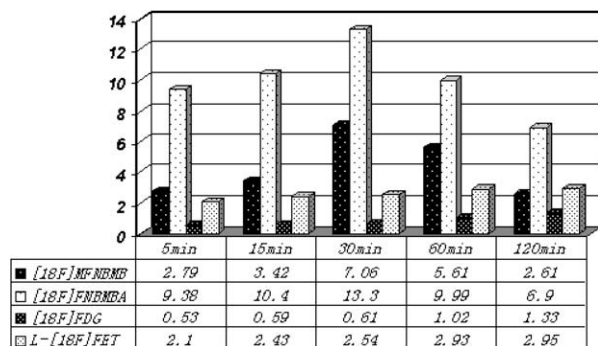


Figure 3. Comparison of tumor-to-brain uptake ratios of [^{18}F]1 and [^{18}F]2 with those of [^{18}F]FDG and L-[^{18}F]FET together in the same animal model bearing S 180 tumor.

and T/M (tumor-to-muscle = 2.62) ratios appeared at the same time point (30 min post-injection) and consequently acid [^{18}F]1 can be better than ester [^{18}F]2 as the imaging agent. On one hand, [^{18}F]1 and [^{18}F]2 showed obvious advantages of biological properties in biodistribution data when compared with [^{18}F]FDG and L-[^{18}F]FET. Besides, the two F-18 labeled fluoroarylvaine derivatives can be easily and efficiently labeled with fluorine-18. Therefore, we expect that the two tracers, especially the acid compound [^{18}F]2, can have potential application in tumor detection, particularly for brain tumor imaging. In conclusion, [^{18}F]FNBMB ([^{18}F]1) and [^{18}F]MFNBMB ([^{18}F]2) designed and synthesized in this study, particularly the acidic F-18 labeled product ([^{18}F]2), demonstrate potential value as more useful PET radiotracers for tumor imaging than [^{18}F]FDG and L-[^{18}F]FET. As an elementary study of [^{18}F]1 and [^{18}F]2 to be the potential PET radiotracers, however, our research on such [^{18}F]fluoroarylvaine derivatives still needs more investigation and further evaluation of them with PET to be better.

Acknowledgments

We acknowledged with thanks for financial supports from the National Natural Science foundation of China (No. 20371009 and 20671014) and Beijing Key Subject Program. We also wish to thank

the cyclotron operator team of the PET Centre of Xuan Wu hospital, for providing [^{18}F]fluoride activity and technical assistance.

References and notes

- Gibson, R. E.; Burns, H. D.; Hamill, T. G.; Eng, W.-S.; Francis, B. E.; Ryan, C. *Curr. Pharm. Des.* **2000**, *6*, 973.
- (a) Weber, W. A.; Avril, N.; Schwaiger, M. *Strahlenther. Onkol.* **1999**, *175*, 356; (b) Delbeke, D. *J. Nucl. Med.* **1999**, *40*, 591; (c) Hoh, C. K.; Seltzer, M. A.; Franklin, J.; deKernion, J. B.; Phelps, M. E.; Beldegrun, A. *J. Urol.* **1998**, *159*, 347; (d) Tang, G. H. *Acta Pharm. Sin.* **2001**, *36*, 470.
- (a) Conti, P. S.; Lilién, D. L.; Hawley, K.; Keppler, J.; Grafton, S. T.; Bading, J. R. *Nucl. Med. Biol.* **1996**, *23*, 717; (b) Engel, H.; Steinert, H.; Buck, A.; Berthold, T.; Huch-Boni, R. A.; von Schulthess, G. K. *J. Nucl. Med.* **1996**, *37*, 441; (c) Strauss, L. G. *Eur. J. Nucl. Med.* **1996**, *23*, 1409.
- Varagnolo, L.; Stokkel, M. P. M.; Mazzi, U.; Pauwels, E. K. *Nucl. Med. Biol.* **2000**, *27*, 103.
- (a) Moon, B. S.; Lee, T. S.; Lee, K. C.; An, G. I.; Cheon, G. J.; Lim, S. M.; Choi, C. W.; Chic, D. Y.; Chuna, K. S. *Bioorg. Med. Chem. Lett.* **2007**, *17*, 200; (b) Martarello, L.; McConathy, J.; Camp, V. M.; Malveaux, E. J.; Simpson, N. E.; Simpson, C. P.; Olson, J. J.; Bowers, G. D.; Goodman, M. M. *J. Med. Chem.* **2002**, *45*, 2250; (c) Jager, P. L.; Vaalburg, W.; Pruijm, J.; de Vries, E. G.; Langen, K. J.; Piers, D. A. *J. Nucl. Med.* **2001**, *42*, 432.
- (a) Wester, H. J.; Herz, M.; Weber, W.; Heiss, P.; Senekowitsch-Schmidtke, R.; Schwaiger, M., et al. *J. Nucl. Med.* **1999**, *40*, 205; (b) Heiss, P.; Mayer, S.; Herz, M.; Wester, H. J.; Schwaiger, M.; Senekowitsch-Schmidtke, R. *J. Nucl. Med.* **1999**, *40*, 1367; (c) Weber, W. A.; Wester, H. J.; Grosu, A. L.; Herz, M.; Dzewas, B.; Feldmann, H. J., et al. *Eur. J. Nucl. Med.* **2000**, *27*, 542.
- Wienhard, K.; Herholz, K.; Coenen, H. H.; Rudolf, J.; Kling, P.; Stocklin, G.; Heiss, W. D. *J. Nucl. Med.* **1991**, *32*, 1338.
- Miura, S.; Murakami, M.; Kanno, I.; Iida, H.; Uemura, K. *Nippon. Rinsho.* **1992**, *50*, 1457.
- Ito, H.; Hatazawa, J.; Murakami, M.; Miura, S., et al. *J. Nucl. Med.* **1995**, *36*, 1232.
- Structure analysis data. F-19 substituted ester 1:* ^1H NMR (500 MHz, CDCl_3): δ 8.28 (m, 1H, Ar-H), 8.15 (dd, $J = 8.6, 1.8$ Hz, 1H, Ar-H), 8.06 (dd, $J = 11.0, 1.8$ Hz, 1H, Ar-H), 7.22–7.19 (m, 1H, NH), 4.82–4.80 (m, 1H, $\text{CHCH}(\text{CH}_3)_2$), 3.82 (s, 1H, OCH_3), 2.35–2.33 (m, 1H, $\text{CH}(\text{CH}_3)_2$), 1.06–1.02 (s, 6H, $\text{CH}(\text{CH}_3)_2$); ^{13}C NMR (125 MHz, CDCl_3): δ 171.87, 161.15, 159.90 (d, 1C, $J_{\text{CF}} = 250.5$ Hz), 150.31, 133.42, 126.58, 119.57, 112.26 (d, 1C, $J_{\text{CF}} = 30.0$ Hz), 57.98, 52.45, 31.46, 19.01, 17.86; ^{19}F NMR (400 MHz, CDCl_3): δ -109.37, -109.40, -109.42, -109.45; MS (EI) m/z : 298.27, found: 299.13; Anal. Calcd for $\text{C}_{13}\text{H}_{15}\text{FN}_2\text{O}_5$: C, 52.35; H, 5.07; N, 9.39. Found: C, 52.73; H, 4.79; N, 9.68. F-19 substituted acid 2: ^1H NMR (500 MHz, CDCl_3): δ 8.31 (m, 1H, Ar-H), 8.17 (dd, $J = 8.5, 2.0$ Hz, 1H, Ar-H), 8.07 (dd, $J = 11.5, 2.0$ Hz, 1H, Ar-H), 7.22–7.18 (m, 1H, NH), 4.87–4.84 (m, 1H, $\text{CHCH}(\text{CH}_3)_2$), 2.46–2.39 (m, 1H, $\text{CH}(\text{CH}_3)_2$), 1.11–1.07 (m, 6H, $\text{CH}(\text{CH}_3)_2$); ^{13}C NMR (100 MHz, CDCl_3): δ 172.91, 163.42, 158.95 (d, 1C, $J_{\text{CF}} = 251.1$ Hz), 149.49 (d, 1C, $J_{\text{CF}} = 9.0$ Hz), 131.52 (d, 1C, $J_{\text{CF}} = 3.6$ Hz), 131.07 (d, 1C, $J_{\text{CF}} = 16.6$ Hz), 119.99 (d, 1C, $J_{\text{CF}} = 3.3$ Hz), 112.38 (d, 1C, $J_{\text{CF}} = 27.5$ Hz), 58.44, 30.18, 19.61, 18.49; ^{19}F NMR (400 MHz, CDCl_3): δ -109.39, -109.42, -109.44, -109.47; MS (EI) m/z : 284.24, found: 284.19; Anal. Calcd for $\text{C}_{12}\text{H}_{13}\text{FN}_2\text{O}$: C, 50.71; H, 4.61; N, 9.86. Found: C, 51.05; H, 4.34; N, 10.13.